Supporting Information

Wang et al. 10.1073/pnas.1210479109

SI Materials and Methods

For in situ hybridization, $Atf5^{+/+}$ and $Atf5^{+/-}$ embryonic stage 18.5 embryos or heads from postnatal day 0 $Atf5^{+/+}$, $Atf5^{+/-}$, and $Atf5^{-/-}$ mice were harvested, fixed in 4% (wt/vol) paraformaldehyde at 4 °C overnight, infused with 25% (wt/vol) sucrose in 1× PBS overnight, embedded in optimal cutting temperature (OCT) compound, and cryosectioned at 18 μm. Digoxigenin-labeled riboprobes against *Atf5* and *LacZ* were used to perform in situ hybridization, as described previously (1).

1. Wang SZ, et al. (2006) An oligodendrocyte-specific zinc-finger transcription regulator cooperates with Olig2 to promote oligodendrocyte differentiation. *Development* 133(17):3389–3398.

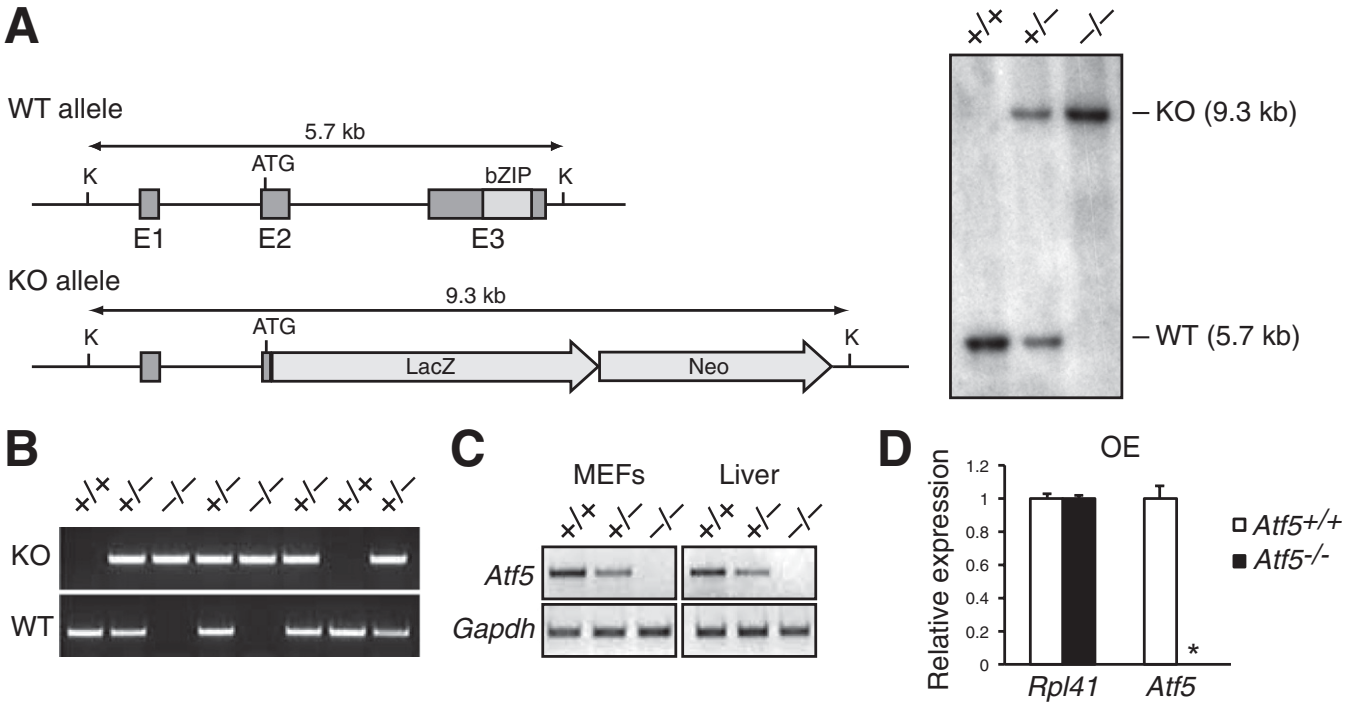

Fig. S1. Validation of $Atf5^{-/-}$ mice. (*A*) (*Left*) Schematic diagrams of the wild-type (WT) and knockout (KO) *Atf5* alleles. To generate the KO allele, a LacZ-Neo cassette was inserted in frame and replaced most of exon 1 (E1) and all of exons 2 and 3 (E2 and E3, respectively). The gene replacement results in an increase in length of a KpnI restriction fragment that encompasses the *Atf5* locus from 5.7 kb (WT allele) to 9.3 kb (KO allele). K represents the KpnI sites; ATG represents the translation start site; bZIP denotes the basic region leucine zipper domain. (*Right*) Southern blot analysis of the *Atf5* locus in $Atf5^{+/+}$, $Atf5^{+/-}$, and $Atf5^{-/-}$ mice. (*B*) PCR genotyping of a litter of $Atf5^{+/+}$, $Atf5^{+/-}$, and $Atf5^{-/-}$ mice from an $Atf5^{+/-}$ intercross. (*C*) RT-PCR analysis of *Atf5* expression in mouse embryonic fibroblasts (MEFs) (*Left*) and liver (*Right*) of $Atf5^{+/+}$, $Atf5^{+/-}$, and $Atf5^{-/-}$ mice. *Gapdh* was monitored as a control. (*D*) qRT-PCR analysis of *Atf5* expression in OE derived from $Atf5^{+/+}$ and $Atf5^{-/-}$ mice. *Rpl41* was monitored as a control. The results were normalized to the expression level in $Atf5^{+/+}$ mice, which was set to 1. $*P < 0.05$.

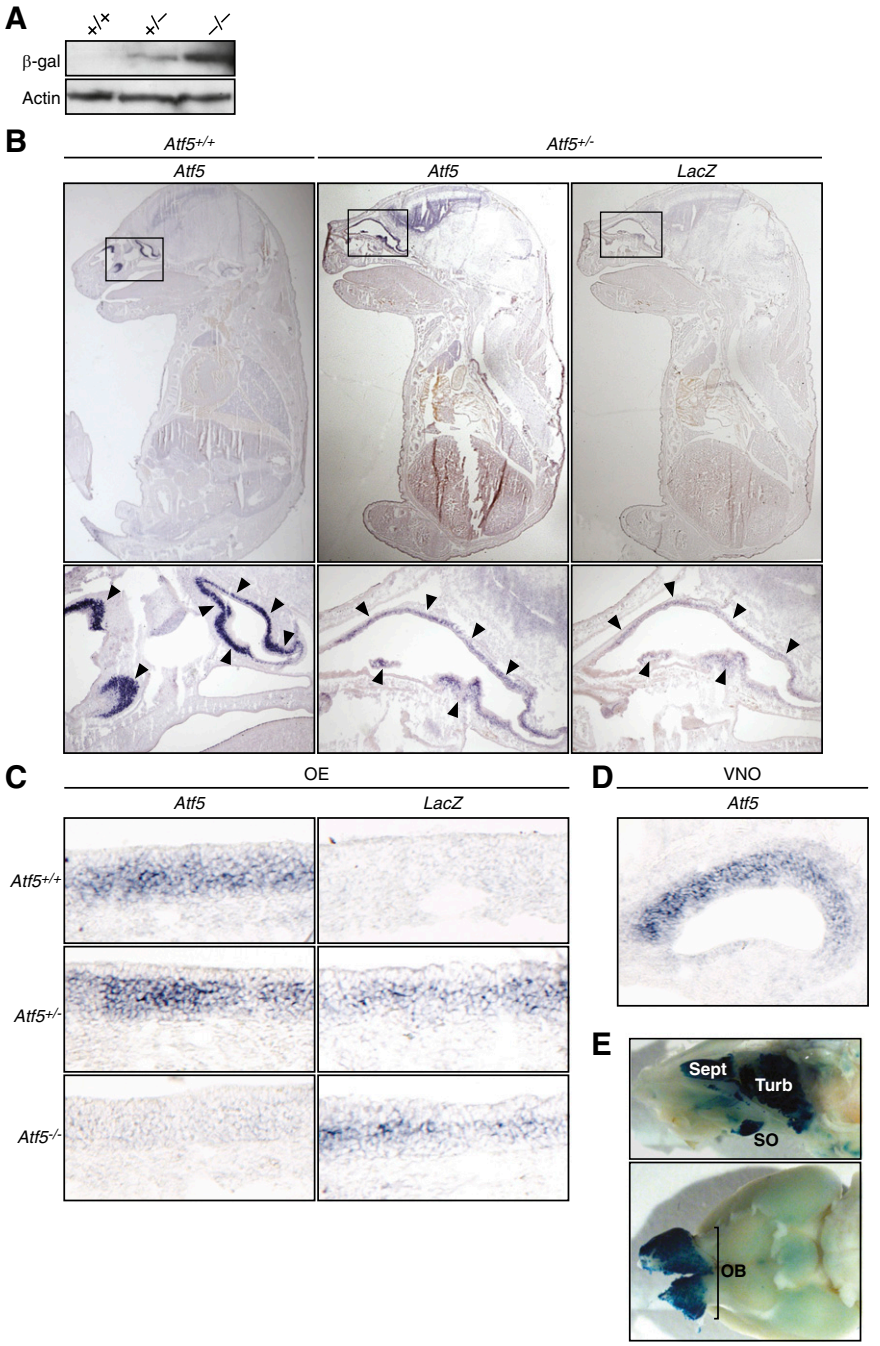

Fig. S2. Further characterization of *Atf5* expression by in situ hybridization analysis and β-gal immunoblot analysis and activity assays. (*A*) Immunoblot analysis monitoring β-gal levels in $Atf5^{+/+}$, $Atf5^{+/-}$, and $Atf5^{-/-}$ mice. Actin was monitored as a loading control. (*B*) In situ hybridization monitoring *Atf5* and *LacZ* expression on a sagittal section of $Atf5^{+/+}$ and $Atf5^{+/-}$ whole embryonic stage 18.5 embryos. *Upper*, magnification 0.8×; *Lower*, magnification 5×. *Inset* highlights the region that is shown in the *Lower* image. Arrowheads denote positive staining. (*C*) In situ hybridization monitoring *Atf5* and *LacZ* expression in the olfactory epithelium (OE) of postnatal day 0 (P0) $Atf5^{+/+}$, $Atf5^{+/-}$, and $Atf5^{-/-}$ mice. Magnification 100×. (*D*) In situ hybridization monitoring *Atf5* expression in the vomeronasal organ (VNO) of a P0 $Atf5^{+/+}$ mouse. Magnification 100×. (*E*) Whole-mount β-gal activity assay on a sagittal section of the nose (*Upper*) and a bottom view of the brain (*Lower*) of a 10-mo-old $Atf5^{+/-}$ mouse. Sept, septum; Turb, turbinates; SO, septal organ; OB, olfactory bulb. Magnification 8×.

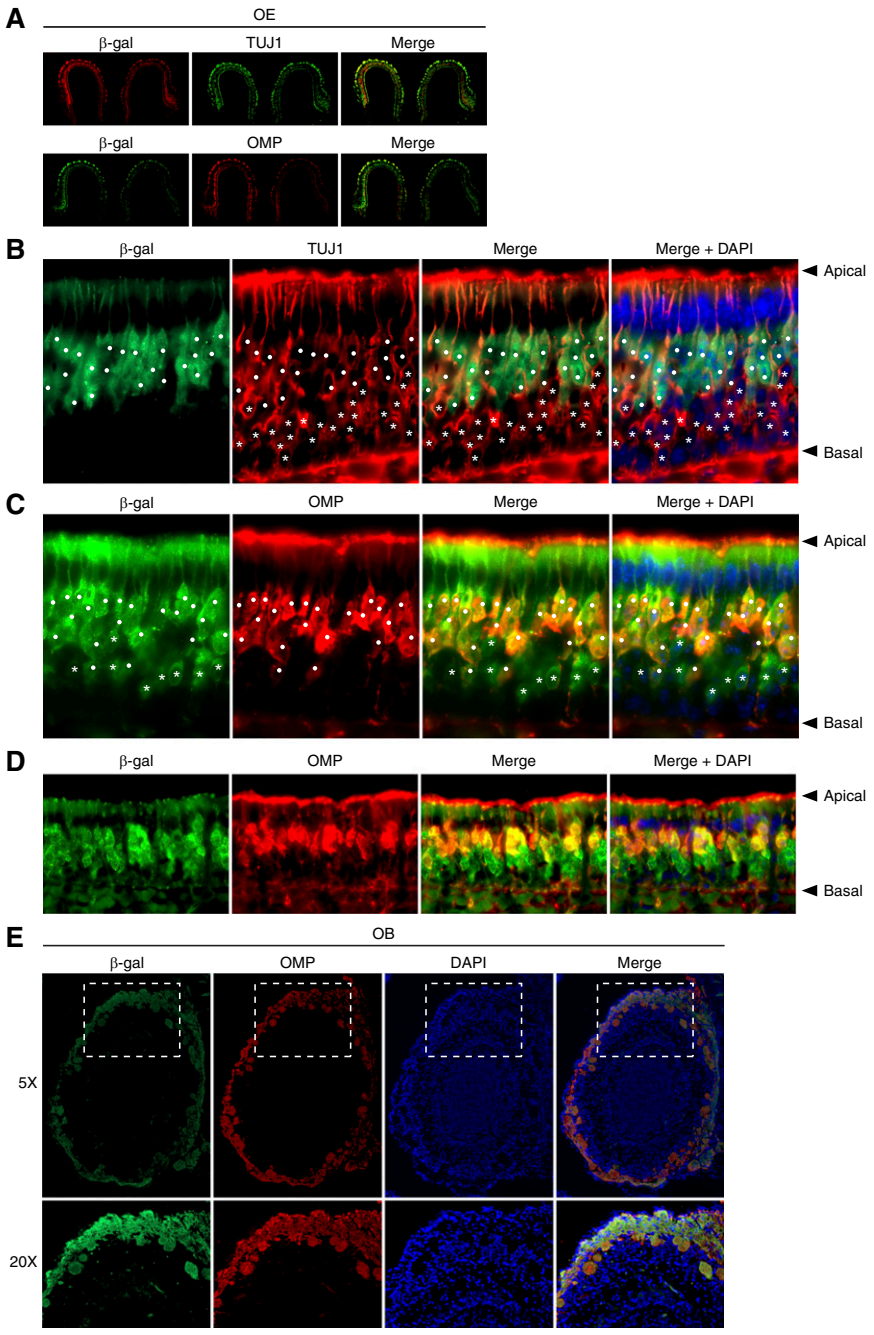

Fig. S3. Immunofluorescence monitoring β-gal and TUJ1, GAP43, and/or OMP staining in the olfactory epithelium (OE) and olfactory bulb (OB). (*A*) Immunofluorescence monitoring β-gal, TUJ1, and OMP staining in the OE of a postnatal day 0 (P0) *Atf5*$^{+/-}$ pup. (*Right*) Merged images. Magnification 5×. The results indicate that *Atf5* is expressed in both immature (TUJ1+) and mature (OMP+) olfactory sensory neurons (OSNs). (*B*) Immunofluorescence monitoring β-gal and TUJ1 staining in the OE of a P0 *Atf5*$^{+/-}$ pup. Merged images are shown in the absence and presence of DAPI. Arrowheads indicate the apical and basal layers of the OE. Magnification 40×. Dots indicate TUJ1+ β-gal+ cells; asterisks indicate TUJ1+ β-gal− cells. The results indicate that many TUJ1+ cells, particularly those located near the basal layer, are β-gal− (asterisks). Significantly, however, some β-gal+ cells also stained strongly for TUJ1 (dots). (*C*) Immunofluorescence monitoring β-gal and OMP staining in the OE of a P0 *Atf5*$^{+/-}$ pup. Merged images are shown in the absence and presence of DAPI. Arrowheads indicate the apical and basal layers of the OE. Magnification 40×. Dots indicate OMP+ β-gal+ cells; asterisks indicate OMP− β-gal+ cells. The results indicate that all OMP+ neurons are also β-gal+ (dots) and that some β-gal+ cells are OMP− (asterisks). (*D*) Immunofluorescence monitoring β-gal and OMP staining in the OE of a 2.5-mo-old *Atf5*$^{+/-}$ mouse. Merged images are shown in the absence and presence of DAPI. Arrowheads indicate the apical and basal layers of the OE. Magnification 40×. (*E*) Immunofluorescence monitoring β-gal and OMP staining in the OB of a P0 *Atf5*$^{+/-}$ pup. Sections were counterstained with DAPI. (*Right*) Merged images. *Upper*, magnification 5×; *Lower*, magnification 20×. (*Upper*) The white dashed box indicates the region that is shown in the *Lower* image. The OMP+, β-gal+ glomerular structures observed in the 20× magnification indicate, as expected, that the β-gal staining in the outer, glomerular layer of the OB is from axons of mature OSNs.

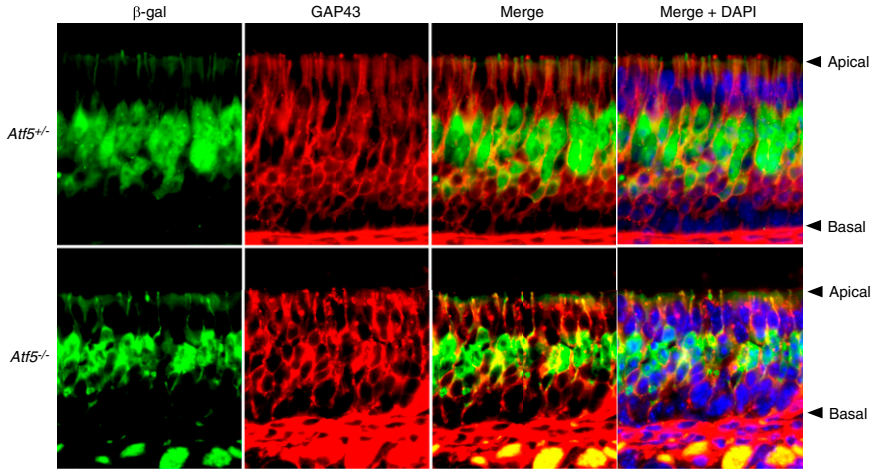

Fig. S4. Immunofluorescence monitoring β-gal and GAP43 staining in the olfactory epithelium (OE) of postnatal day 0 *Atf5*$^{+/-}$ and *Atf5*$^{-/-}$ mice. Merged images are shown in the absence and presence of DAPI. Arrowheads indicate the apical and basal layers of the OE. Magnification 40×. The results are consistent with those obtained by TUJ1 staining and show that *Atf5* is expressed in some but not all immature olfactory sensory neurons.

Fig. S5. Identification of genes with decreased expression in *Atf5*$^{-/-}$ olfactory epithelium (OE). Heat map displaying the 274 genes whose expression level was significantly decreased in *Atf5*$^{-/-}$ OE (green) relative to that in *Atf5*$^{+/+}$ OE (red). In addition, there were seven genes whose expression level was increased in *Atf5*$^{-/-}$ OE relative to that in *Atf5*$^{+/+}$ OE (Dataset S1).

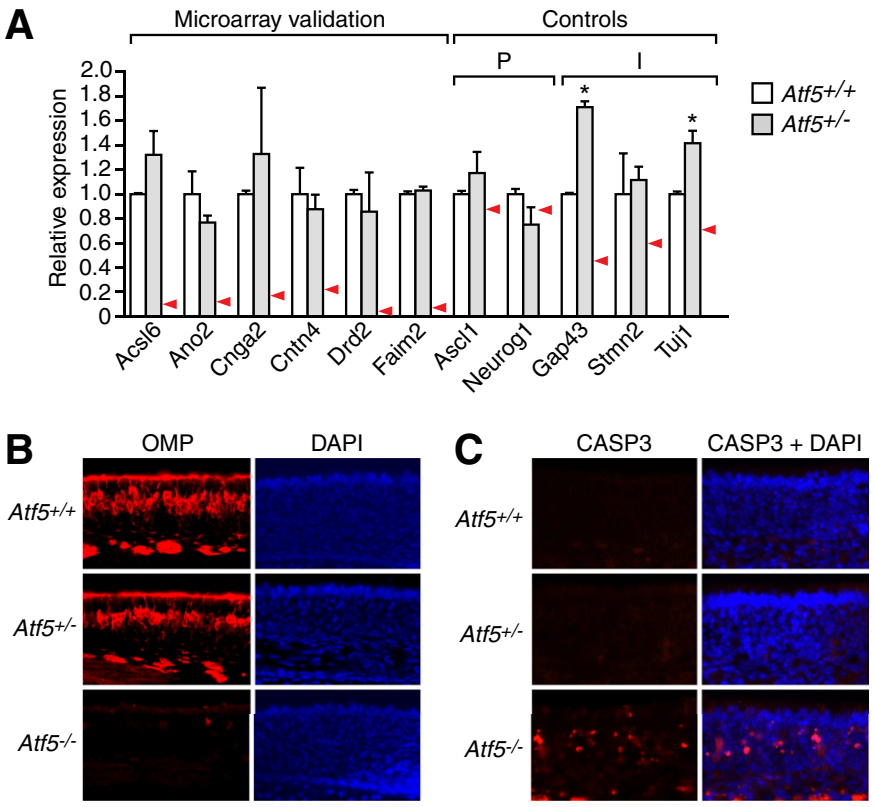

Fig. S6. Similarity in olfactory sensory neuron (OSN)-specific gene expression and OMP and cleaved caspase 3 (CASP3) staining between *Atf5*$^{+/+}$ and *Atf5*$^{+/-}$ mice. (*A*) qRT-PCR analysis monitoring gene expression in olfactory epithelium (OE) of postnatal day 0 (P0) *Atf5*$^{+/+}$ and Atf5$^{+/-}$ mice. The results were normalized to the expression level in *Atf5*$^{+/+}$ mice, which was set to 1. Red arrowheads indicate the relative expression of each gene in *Atf5*$^{-/-}$ mice, as shown in Fig. 4*B*. P, progenitor markers; I, immature OSN markers. *$P < 0.05$. The results show that expression of OSN-specific genes was similar in *Atf5*$^{+/+}$ and *Atf5*$^{+/-}$ mice. (*B*) Immunofluorescence monitoring OMP staining in the OE of P0 *Atf5*$^{+/+}$, *Atf5*$^{+/-}$, and *Atf5*$^{-/-}$ mice. (*Right*) DAPI images. Magnification 20×. (*C*) Immunofluorescence monitoring cleaved CASP3 staining in the OE of P0 *Atf5*$^{+/+}$, *Atf5*$^{+/-}$, and *Atf5*$^{-/-}$ mice. Merged images are shown in the absence and presence of DAPI. Magnification 20×.

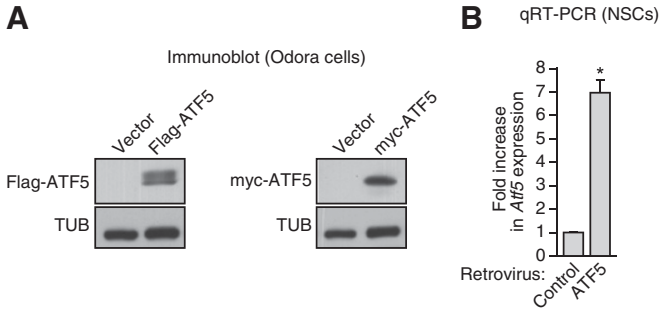

Fig. S7. Confirmation of ectopic *Atf5* expression. (*A*) Immunoblot analysis monitoring Flag-ATF5 (*Left*) and myc-ATF5 (*Right*) levels in rat Odora cells transfected with empty vector and Flag-ATF5 or myc-ATF5. Tubulin was monitored as a loading control. (*B*) qRT-PCR analysis monitoring expression of *Atf5* in mouse neural stem cells (NSCs) transduced with a retrovirus that expresses ATF5 or empty virus control. Fold increase in *Atf5* expression is given relative to the empty virus control, which was set at a value of 1. *$P < 0.05$.

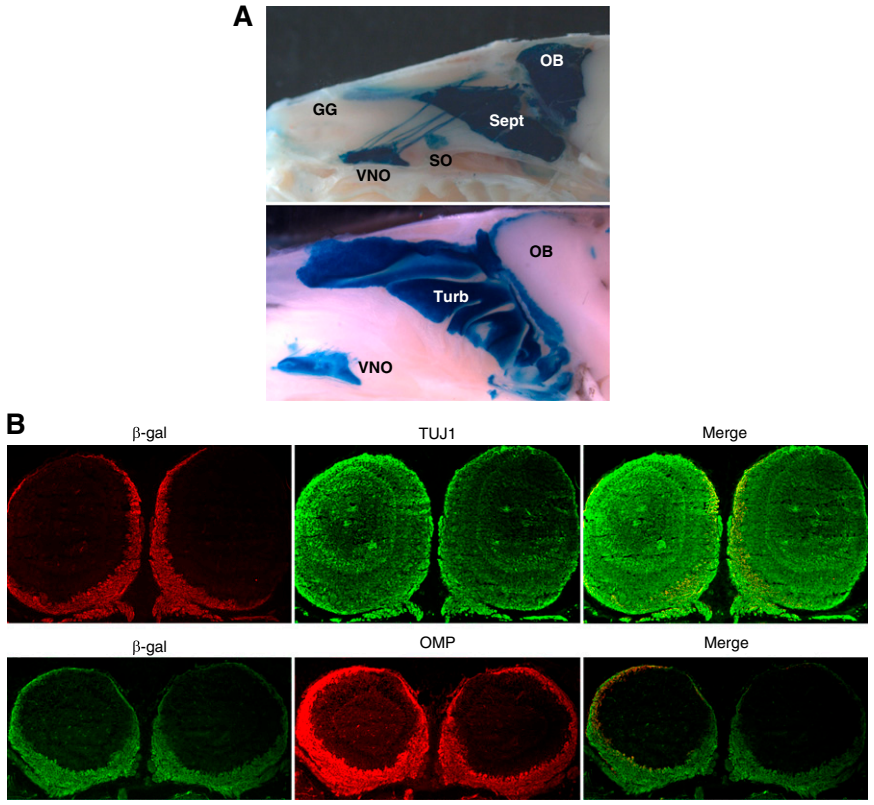

Fig. S8. Enlarged versions of images shown in Fig. 2*A* and Fig. 3*D*. (*A*) From Fig. 2*A*. Whole-mount β-gal activity assay on two different sagittal head sections of a P30 *Atf5*$^{+/-}$ mouse. GG, Grueneberg ganglion; OB, olfactory bulb; Sept, septum; SO, septal organ; Turb, turbinates; VNO, vomeronasal organ. Magnification 5×. (*B*) From Fig. 3*D*. Immunofluorescence monitoring β-gal, TUJ1, and OMP staining in coronal sections of the OB of a postnatal day 0 *Atf5*$^{+/-}$ pup. (*Right*) Merged images. Magnification 50×.

Other Supporting Information Files

Dataset S1 (XLS)